



Microstructural evolution during low-temperature TLP bonding of WC-6Co cemented carbide to AISI 1045 steel using multi-layer of Ni/Cu/In/Cu/Ni

Saeid Nahri¹ · Reza Tavangar¹

Received: 25 July 2024 / Accepted: 31 August 2024
© International Institute of Welding 2024

Abstract

Transient liquid phase (TLP) bonding of WC-6Co cemented carbide to 1045 steel was performed using a selected Ni/Cu/In/Cu/Ni multi-interlayer at low temperature of 650°C for three different holding times of 10, 20, and 30 min. The Cu and Ni layers were electro deposited on the joining surface of both substrates to prepare the interfaces for joining. Then, an indium film with thickness of 5 µm was settled between them as an interlayer to form the Cu-In solid solution via TLP process. For a bonding time of 10 min, isothermal solidification of copper solid solution was incomplete and double-phase microstructure of δ-(Cu) was formed, but it was observed that by prolonging the TLP holding time to 30 min, due to a rather completing of homogenization of the isothermally formed Cu-In solid solution in joint area, the maximum shear strength of 173 MPa was obtained.

Keywords Transient liquid phase · Dissimilar bonding · WC-Co cermet · Shear strength · Indium

1 Introduction

Cemented carbides, such as WC-Co, are a family of composite materials comprising a hard ceramic material (tungsten carbide) and a ductile metal binder (cobalt) [1]. These materials are widely used to manufacture cutting dies, material-deforming tools, structural components, mining bits, and press molds due to their high hardness and superior wear and abrasion resistance [2]. However, the high production costs and significantly lower fracture toughness of cemented carbides often limit their use to the cutter tips, which are joined to steel stems in most cutting tools. Various welding methods, such as fusion welding, brazing, and diffusion bonding, have been explored to weld WC-Co and steel, addressing challenges like significant differences in the coefficient of thermal expansion (CTE), the formation of brittle η phases (e.g., Fe₃W₃C and Co₆W₆C) [3, 4], and the creation of a cobalt-depleted zone (CDZ) due to excessive cobalt diffusion from the cemented

carbide to the molten weld zone [5]. Efforts have been made to eliminate brittle phases and reduce residual stresses when welding cemented carbide to steel.

Fusion welding procedures, due to their high heat input, can result in unfavorable complex reactions in the molten pool. Previous studies observed the formation of various brittle η phases, such as Fe₃C, Fe₃W₃C, and Co₃W₃C, at the joint interface due to the diffusion of decomposed tungsten and carbon from the cemented carbide into the molten pool, thereby deteriorating the joint's strength and toughness [6, 7]. It was also reported that elevated temperatures during fusion welding can lead to the growth of WC particles [8]. Additionally, volume changes during the cooling process, caused by potential phase transformations in the steel component, can increase the risk of crack propagation [9]. Thus, bonding temperatures above the phase transformation temperature of steel negatively impact the final mechanical properties of the joint specimens.

Among the various methods, brazing has demonstrated better efficacy than fusion welding for joining cemented carbide and steel, owing to the superior quality of the brazed joints and lower overall costs. The brazing method reduces intense deformation and residual stresses from the non-uniform heating seen in fusion welding processes. However, the formation of brittle compounds or cobalt depletion from the cemented carbide due to excessive diffusion into the liquid filler remains

Recommended for publication by Commission XVII - Brazing, Soldering and Diffusion Bonding

✉ Saeid Nahri
SaeidNahri.MaterialEng@gmail.com

¹ Department of Materials Engineering, Sahand University of Technology, P.O.Box: 51335-1996, Tabriz, Iran

common in brazing, adversely affecting the joint's toughness [10]. Zhang et al. [5] brazed WC-8Co/SAE1045 steel using various Cu-Ni-Al fillers and found that intense diffusion and reactions between the molten filler alloy and the WC-8Co component created a CDZ-destroyed layer at the cemented carbide interface, leading to microcrack propagation. They reported that Cu from the filler alloy and Fe from the steel, diffused into the molten filler metal, attracted cobalt from the WC-Co side into the joint, causing CDZ. Habibi et al. [10] proposed brazing WC-Co to steel at a low temperature (650°C) using a silver-based filler metal to avoid CDZ. However, even at this temperature for 10 min, the formation of Co-Fe-Cu based reaction products could not be avoided, resulting in CDZ. Additionally, the service temperature of brazed joints is limited due to the segregation of low melting-point elements or eutectic in the brazing seam [11–13]. In brazing, the maximum service temperature is generally estimated to be around 0.5 T_m of the filler metals [14].

Diffusion bonding is an alternative method to join cemented carbides, performed in a solid state to mitigate harmful phase formation and residual stress in the joint area [15, 16]. Feng et al. [17] and Barrena et al. [18] demonstrated that using pre-sintered Ni and composite Cu/Ni interlayers can improve the reliability of diffusion-bonded carbide and steel joints by relieving residual stress through plastic deformation. Additionally, η phases and CDZ were effectively eliminated since the Ni interlayer blocks both Cu and Fe from the WC-Co surface [15, 19, 20]. Li et al. [21] compared Co and Ni/Co interlayers and reported that using nickel reduced residual stresses and prevented excessive cobalt diffusion and η phase formation even at bonding temperatures of 1000°C and bonding times of 1 h, unlike Co interlayers. Although diffusion bonding joints exhibit advantages such as minimal thermal damage to base materials and suitability for high-temperature applications [6, 7], its use is limited to simple geometries and requires primary preparation of the joint surfaces, leading to higher costs [22].

Transient liquid phase (TLP) bonding is considered a hybrid joining process that combines characteristics of liquid-phase bonding and diffusion bonding to leverage the benefits of both techniques. In TLP bonding, a molten filler metal initially fills the joint, then diffuses into the substrates during the heating stage to form a solid solution containing elements from both the interlayer and substrates [23]. Unlike brazing, in TLP bonding, the remelting point of the formed joint is higher than the bonding process temperature, making it suitable for high-temperature applications. Furthermore, since the molten interlayer wets the contact surfaces in TLP bonding, significant axial loading is not required to form proper bonds, unlike diffusion bonding [24]. Guo et al. [25] performed TLP bonding of WC-Co cemented carbide to steel using a Ti/Ni/Ti multi-interlayer at 950–1100°C and obtained a maximum shear strength of about 137 MPa. In

another study, Zeidabadinejad et al. [26] managed to bond WC-Co to St52 steel at 1200°C using a pure copper interlayer via the TLP method. They observed a 10- μm -thick CDZ for the shortest bonding time (1 min) and reported that prolonging the bonding time increased the CDZ thickness to about 30 μm and caused microcracks in the absence of the cobalt binder. This study further evidenced the destructive effect of Cu and Fe in brazing WC-Co to steel.

This study aims to achieve joints free of brittle phases, avoid CDZ, and minimize residual stresses by reducing the bonding temperature while achieving a higher remelting point. To this end, the conventional brazing treatment of WC-Co to steel using silver-based filler alloys is replaced by the TLP bonding method using a multilayer of Ni/Cu/In/Cu/Ni. In this novel configuration, a Ni electrodeposit layer on WC-Co is used to prevent CDZ and the formation of undesired compounds like η phases. The Cu-In system is proposed to perform the bonding procedure at a low temperature of 650°C (below the phase transformation temperature of the steel) while achieving a higher remelting point, which is not possible with silver-based alloys. This study investigates the microstructure of the interfaces of WC-Co/Ni/Cu and steel/Ni/Cu. The effects of bonding time on microstructural evolution and mechanical properties of the joint are evaluated, and the fracture behavior and mechanism under shear load are elucidated.

2 Experimental procedure

2.1 Starting materials

Cylindrical specimens of WC-6Co cemented carbide and 1045 steel, each with a diameter of 8 mm, were cut to lengths of 2 mm and 11 mm, respectively. The chemical composition of the materials used was as follows:

Steel (1045): C: 0.45%, Mn: 0.6%, P: 0.04%, S: 0.05%, Fe: balance.

Cemented carbide (WC-6Co): C: 5.87%, W: 88.03%, Co: 6.1%.

Before performing the TLP treatment, nickel and copper coating layers with thicknesses of approximately 5 and 45 μm , respectively, were electrodeposited on the joining surfaces of both the steel and cemented carbide specimens. A core indium interlayer with a thickness of 5 μm was then placed between the Ni/Cu coated surfaces of the components, as shown in Fig. 1.

Unlike systems such as Cu-Fe [25] or Ni-Ti [26], which were previously used as interlayers for TLP bonding of carbide to steel, the TLP joining process using Cu and In interlayers can be performed at lower temperatures. However, copper, unlike nickel, has very low solubility in Co and Fe. This is why a nickel coating was initially applied to the

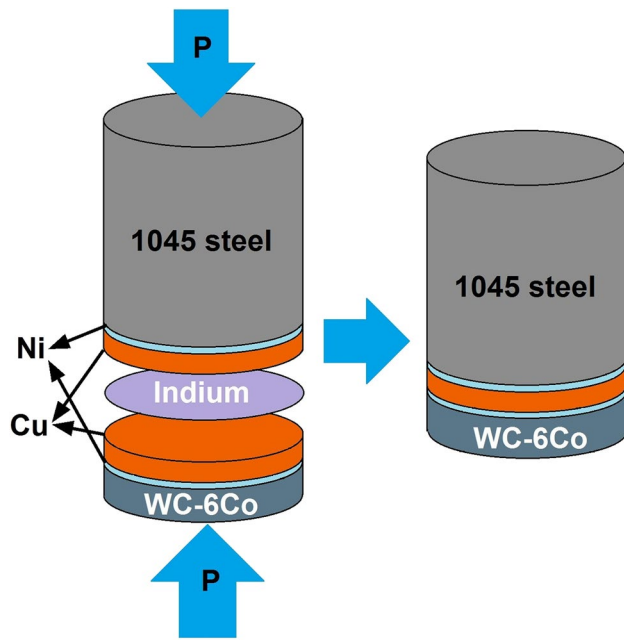


Fig. 1 Schematic representation of the settled intermediate layers as well as indium interlayer used for TLP bonding process

polished and degreased substrates, due to its high physical and chemical affinity to both Co (on the cemented carbide side) and Fe (on the steel side). Nickel was electroplated on the bonding surfaces of both the cemented carbide and steel specimens using Watts electrolyte (250 g/l $\text{NiSO}_4 \cdot 6\text{H}_2\text{O}$, 45 g/l $\text{NiCl}_2 \cdot 7\text{H}_2\text{O}$, 45 g/l H_3BO_3 , 3 g/l saccharin, 0.05 g/l sodium dodecyl sulfate) with a pH of 3.5 and a current density of 0.1 A/m^2 at 45°C . For electroplating copper onto the nickel-coated surfaces of the specimens, a copper sulfate electrolyte with a pH of 4 was used under a cathode current of 0.1 A/m^2 at 25°C .

2.2 Joining procedure

The coated substrates and Indium interlayer foil were cleaned in acetone and then assembled in a graphite mold, as shown in Fig. 1. The bonding was performed in a vacuum furnace at 10^{-3} Pa . To prevent movement of the assembled parts, a small weight, producing a compressive stress of about 0.3 MPa, was placed on the upper side of the settlement. The samples were heated to the targeted bonding temperature of 650°C at a rate of 20°C/s and held at this temperature for 10, 20, and 30 min. This TLP process can form a Cu(In) solid solution. The initial bonding time was set at 10 min, with 10-min increments added to determine the required time to form a solid solution containing less than 4% indium (atomic percent), which, according to the Cu-In phase diagram, has a relatively high re-melting point. After the TLP process, the samples were cooled in the furnace to ambient temperature.

Since the formation of intermetallic compounds slows down the diffusion rate and increases the bonding time [23, 27], the temperature of the TLP process was set at 650°C , above which no intermetallic compounds are formed.

2.3 Microstructure characterization and mechanical testing

Ambient temperature shear tests were conducted to evaluate the shear strength of the TLP joint specimens under a cross-head speed of 0.5 mm/min using a GOTECH AI-7000-IA10 testing machine. Each reported value for the shear strength is the average of three test results. Variations in the microhardness of the TLP joints, including the intermediate coated layers, were measured using a microhardness tester (model Mdpel M400) with a 50-g load. To study the microstructure of the joints, metallographic samples were prepared from the cross-section of the joint area. The samples were ground using a 100–3000-grit waterproof SiC grinding paper. An Olympus PMG3 optical microscope (OM) was used for the microscopic examination of the samples. A scanning electron microscope (model: VEGA Tscan) equipped with an energy-dispersive spectrometry system (RÖNTEC) was used to observe the interfacial microstructure, conduct chemical analysis of the microstructural phases in the joint area, and examine the fracture surface of the shear test specimens. For phase analysis, the joint area and fractured surfaces were studied using an X-ray diffractometer (model: Bruker Axo-Advance D8) with a $\text{K}\alpha\text{-Cu}$ wavelength.

3 Results and discussions

3.1 Microstructure of diffusion zone

Figure 2 presents the SEM micrographs of the as-polished WC-6Co/Ni/Cu/In/Cu/Ni/steel joint after 10 min of TLP bonding at 650°C . In Fig. 2b and e, which are higher magnifications of the TLP bonded areas from Fig. 2a and d, a dual-phase composition is evident. Based on the EDS results of the marked phases (denoted in Fig. 2b) and the XRD diffraction spectra from the joint (Fig. 3), collected from the sample bonded for 10 min, it appears that isothermal solidification of copper solid solution with less than 4% indium (atomic percent) was not completed and during cooling from the bonding temperature (650°C), according to the Cu-In phase diagram, the indium-rich β phase underwent a eutectoid reaction at approximately 574°C , transforming into a dual-phase-layered microstructure of δ intermetallic compound (as the matrix phase) and particles of (Cu) solid solution. Figure 2c represent EDS element mapping of dual-phase microstructure in Fig. 2b which clearly show higher concentration of indium in dual-phase microstructure compare to adjacent areas. The

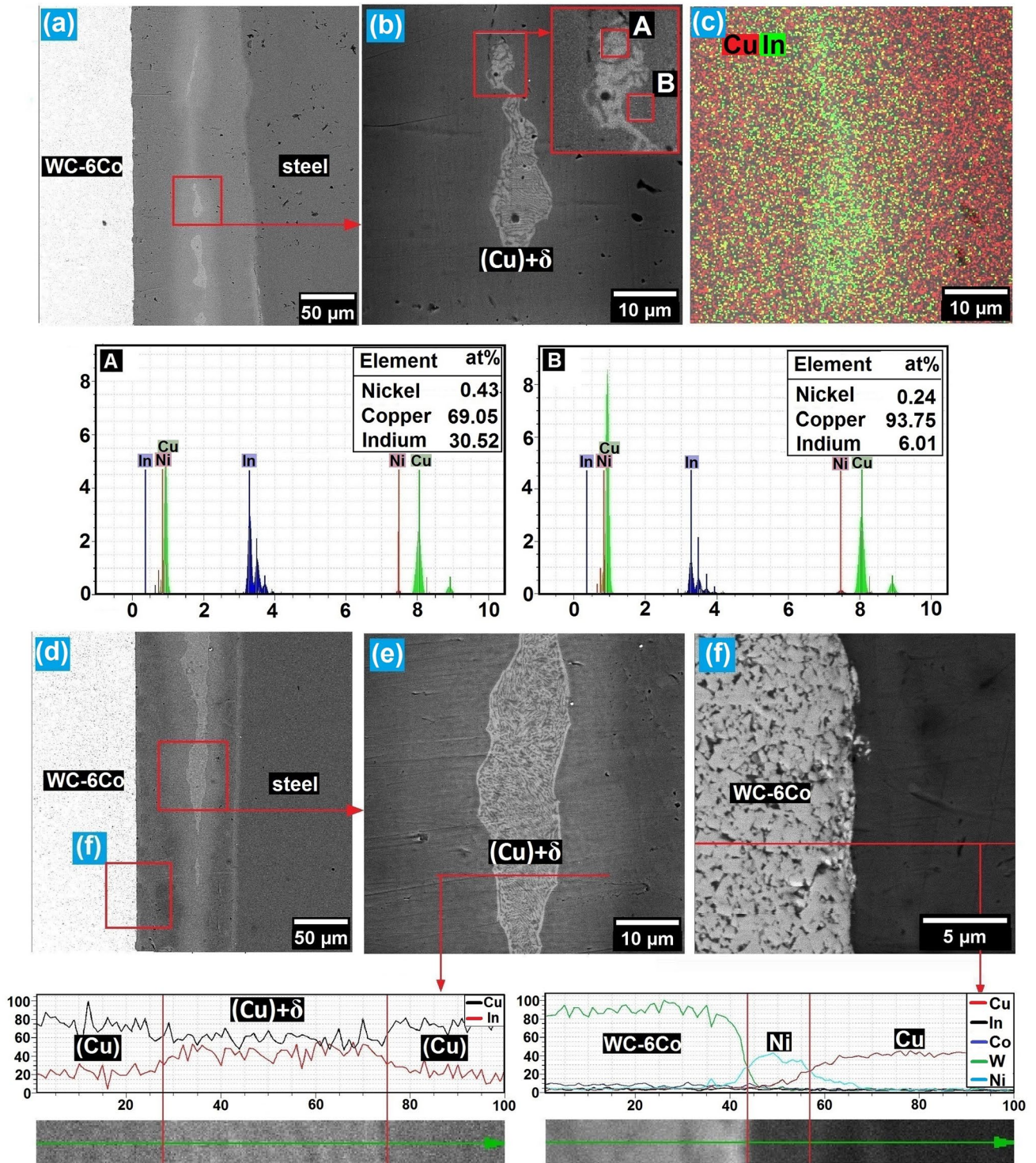


Fig. 2 SEM images, EDS mapping, EDS analyses, and concentration profiles from joint area and WC-6Co/Ni/Cu interfaces of the sample bonded at 650°C for 10 min

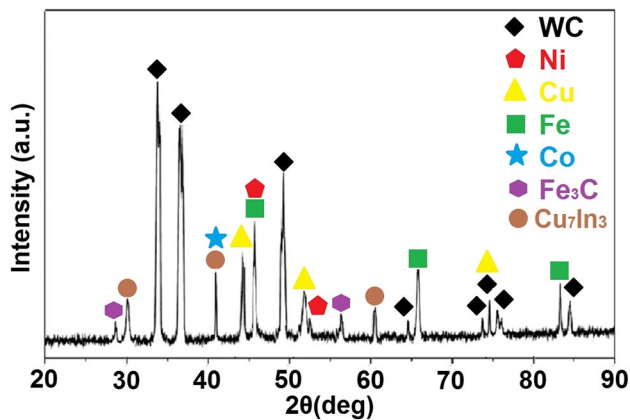


Fig. 3 XRD pattern from joint area of the sample bonded at 650°C for 10 min

concentration profile of the dual-phase microstructure of δ and (Cu) in Fig. 2e also indicates a high concentration of indium compared to the adjacent areas. Although the desired composition of the copper solid solution with less than 4% indium was not achieved through isothermal solidification, 10 min was sufficient for a significant amount of inter-diffusion of elements at the WC-6Co/Ni/Cu interfaces, as evidenced by the concentration profile in Fig. 2f.

Figures 4 and 5 demonstrate the OM micrograph and SEM images of the TLP joint after a bonding time of 20 min. In Figs. 4 and 5a, a single-phase microstructure with a low concentration of indium has formed, as indicated by EDS analysis at point C. This signifies the completion

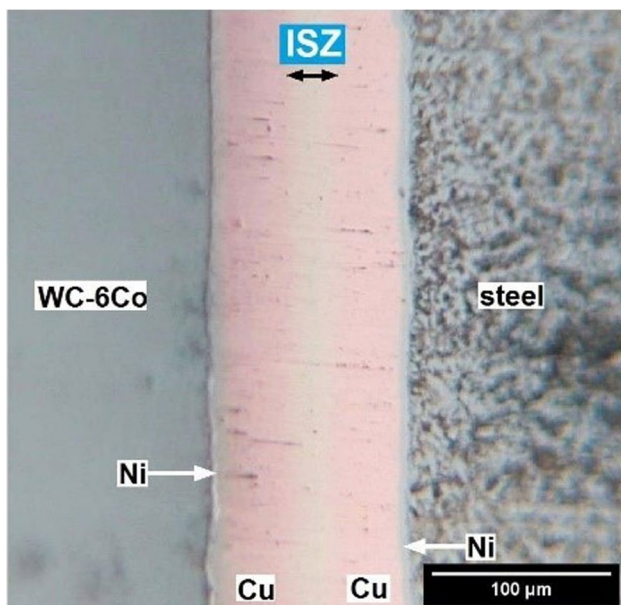


Fig. 4 OM image from joint area of the sample bonded at 650°C and 20 min

of isothermal solidification of copper solid solution. Therefore, a bonding time of 20 min was sufficient for the isothermal solidification of a copper solid solution with less than 6% atomic percent indium. Figure 5b and c shows higher magnifications of the WC-Co/Ni/Cu and Cu/Ni/Steel interfaces, respectively. These images reveal sound joints at the interfaces, and the concentration profiles indicate significant inter-diffusion of elements. However, due to the one-unit difference between copper and nickel in atomic number, the Cu/Ni interface is not distinguishable.

Figure 6 presents the SEM images and concentration profiles, of the TLP joint and interfaces for a specimen bonded for 30 min at a constant temperature of 650°C. Although isothermal solidification was completed for the joint bonded at 650°C for 20 min, the bonding time was prolonged to 30 min to achieve a higher re-melting point and consequently a higher service temperature by decreasing the indium concentration in the joint area. Based on the EDS analysis presented in Fig. 7b collected from point D marked in Fig. 6a and binary system of Cu-In [28] (Fig. 7a), an alloy with less than 4% indium (atomic percent) will have re-melting point higher than 900°C. This decrease allowed for a higher melting point to be achieved despite maintaining the bonding temperature at 650°C, which is below the phase transformation temperature of AISI 1045. According to Fig. 6b, c and the element concentration profiles from the interfaces, prolonging the bonding time promoted the diffusion of elements. However, as expected, due to the stability of WC at the bonding temperature, no interaction between W, C, and Ni occurred, which is well established by the XRD spectra of the TLP joint formed after 30 min (Fig. 8). Furthermore, no Cu-In intermetallic compound was detected in Fig. 8, which provides additional evidence for the isothermal solidification of copper solid solution with less than 4% indium.

Figure 9 shows higher magnifications of the WC-6Co/Ni/Cu interfaces of the joint TLP bonded for 30 min. In Fig. 9a and previous SEM images of the cemented carbide interfaces, there is no evidence of a cobalt depletion zone (CDZ) when compared to studies by Habibi et al. [10] and Hang et al. [5], which both reported at least a 5- μ m-thick CDZ on the WC-Co side. The concentration profile of elements in Fig. 9b illustrates a rather homogeneous distribution of cobalt in the WC-6Co side. EDS analysis at points E and F in Fig. 9b confirms the presence of cobalt on the cemented carbide side of the interface, providing further evidence of a CDZ-free joint. It is also important to note that the formation of brittle compounds such as η phases was avoided. Comparing the compositions at points E and F with the compositions of η phases such as $\text{Fe}_3\text{W}_3\text{C}$ and $\text{Co}_6\text{W}_6\text{C}$, which typically form at the cemented carbide

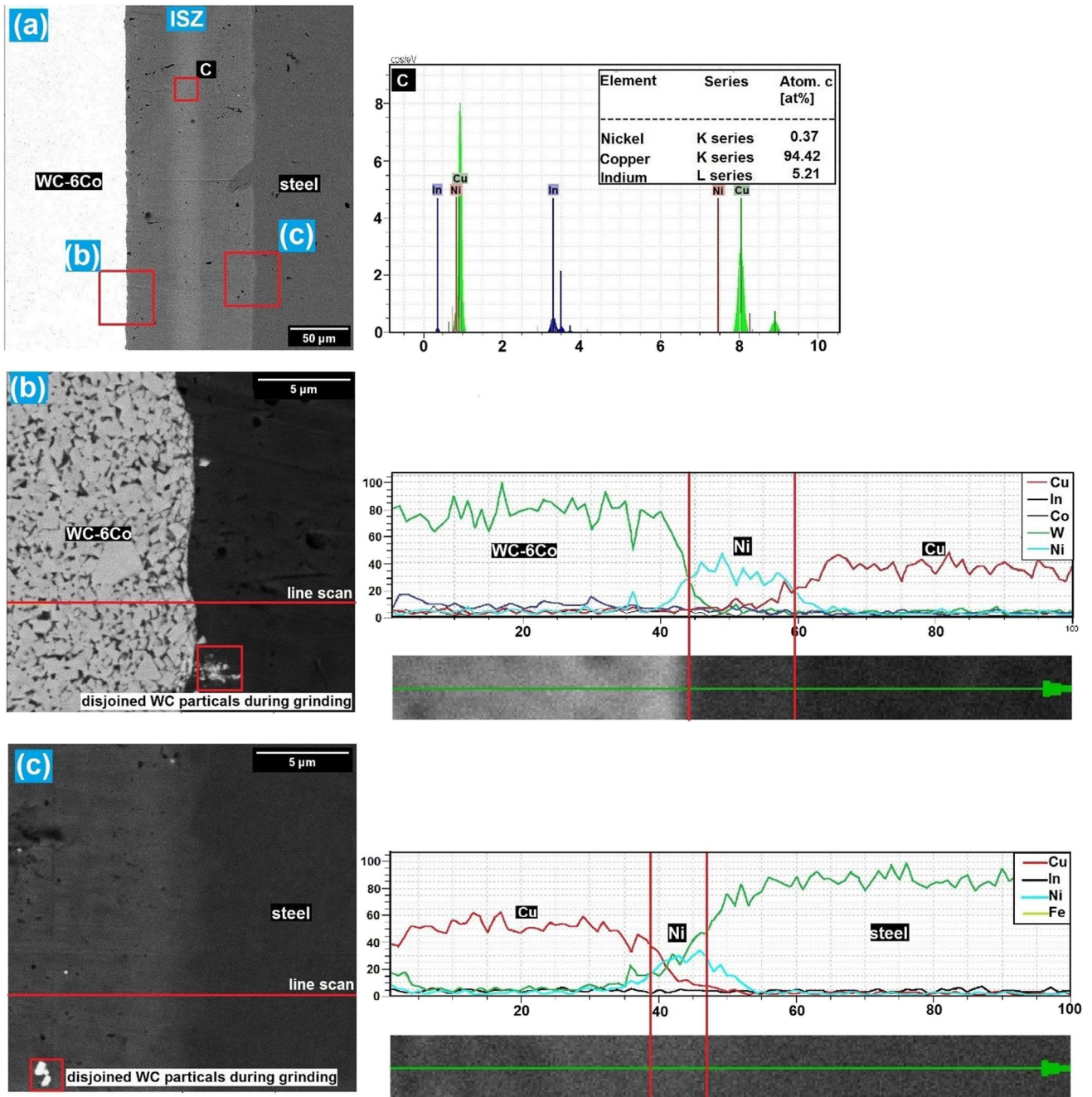


Fig. 5 SEM images, EDS analysis, and concentration profiles from joint area, WC-6Co/Ni/Cu and Cu/Ni/steel interfaces of the sample bonded at 650°C for 20 min

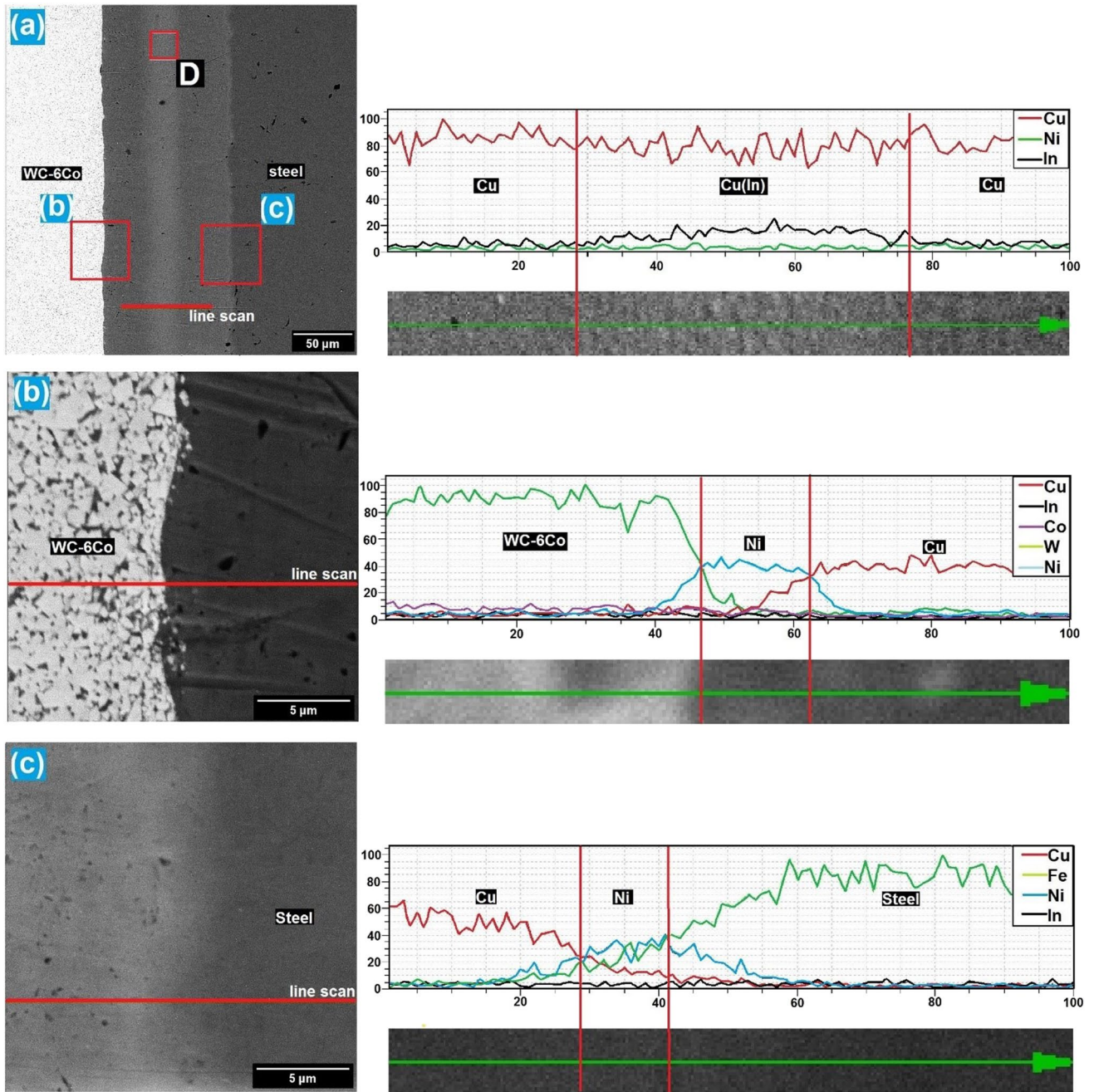


Fig. 6 SEM images and concentration profiles from joint area, WC-6Co/Ni/Cu, and Cu/Ni/steel interfaces of the sample bonded at 650°C and 30 min

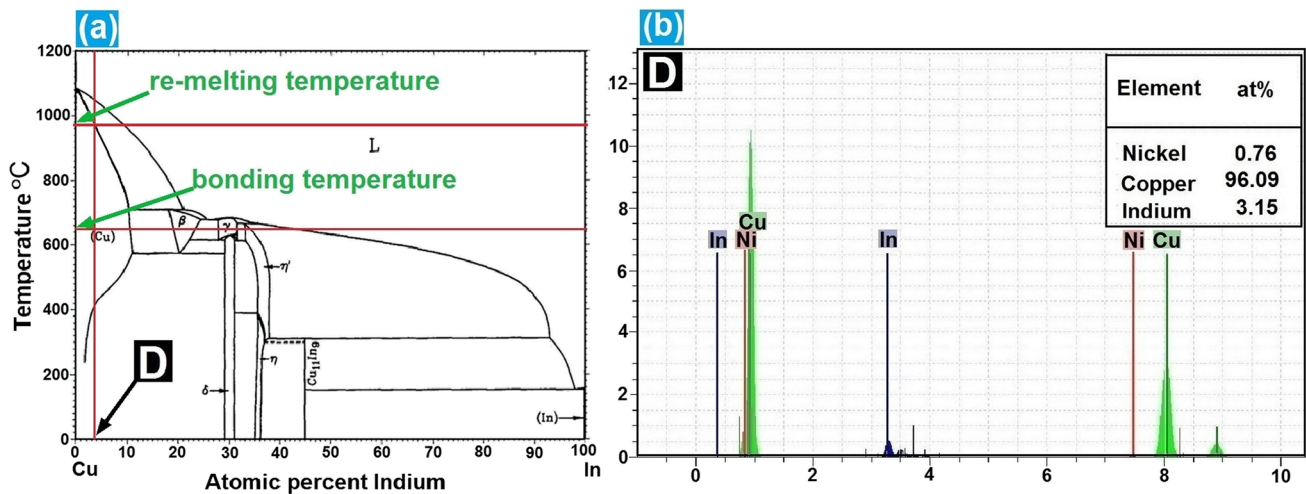


Fig. 7 a Cu-In phase diagram [28], b EDS analysis from point D marked in Fig. 5a

interface with filler alloys [3, 4], confirms this. Li et al. [21] reported that the ultimate phase at the WC–Co/Ni interface was WC + (Ni, Co) solid solution for all samples diffusion bonded at three temperatures (950, 1000, and 1050°C) for 1 h while for WC–Co/Co configuration they observed a 2.3- μm -thick $\text{Co}_6\text{W}_6\text{C}$ at the interface of WC–Co with cobalt interlayer.

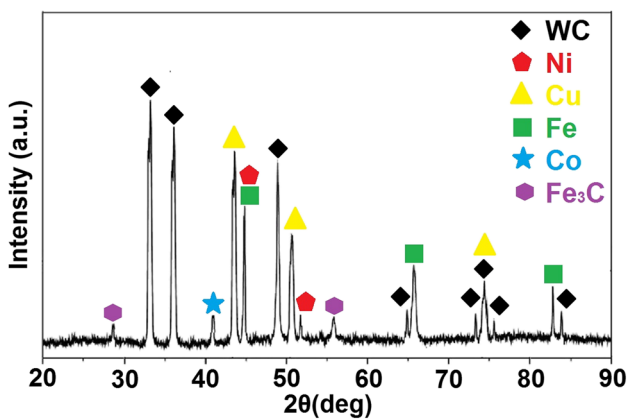


Fig. 8 XRD pattern from joint area of the sample bonded at 650°C for 30 min

3.2 Mechanical properties

3.2.1 Micro-hardness measurements

The hardness measurements for each specimen were performed at seven points within the joint area. One of these points was in the center of the joint area, and two were adjacent to the joint area. The other measurements were taken at the intermediate layers. As shown in Fig. 10, the maximum microhardness value in the center of the joint area is associated with a bonding time of 10 min, which is attributed to the double-phase microstructure of δ and (Cu) in the joint center of this sample. In samples bonded for 30 min, rather homogeneous microhardness values are evident across the joint area, indicating a uniform Cu-In solid solution throughout the joint. It should be noted that the hardness in the center of the joint area in samples bonded for 20 and 30 min is higher than that in both copper intermediate layer sides, owing to the Cu-In solid solution strengthening effect. Additionally, as the bonding time increased from 10 to 30 min, the overall hardness of the copper intermediate layer and ISZ decreased to about 68 HV, which is comparable to the hardness of pure coated copper. Thus, it can be deduced that the overall inter-diffusion of elements has only a small impact on the hardness and shear strength of the joints.

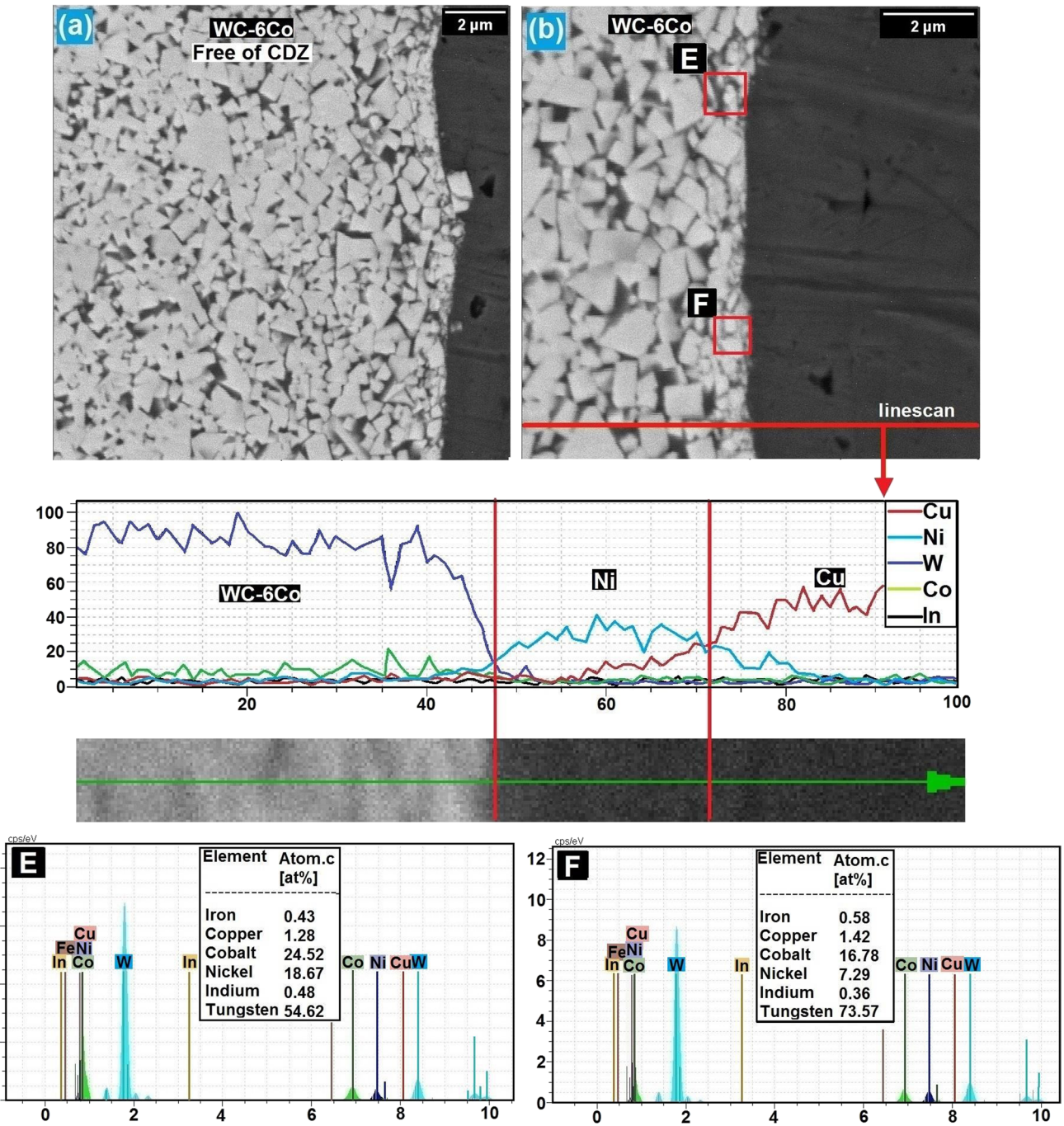


Fig. 9 SEM images, EDS analyses, and concentration profile of WC-6Co/Ni/Cu interfaces of sample bonded for 30 min

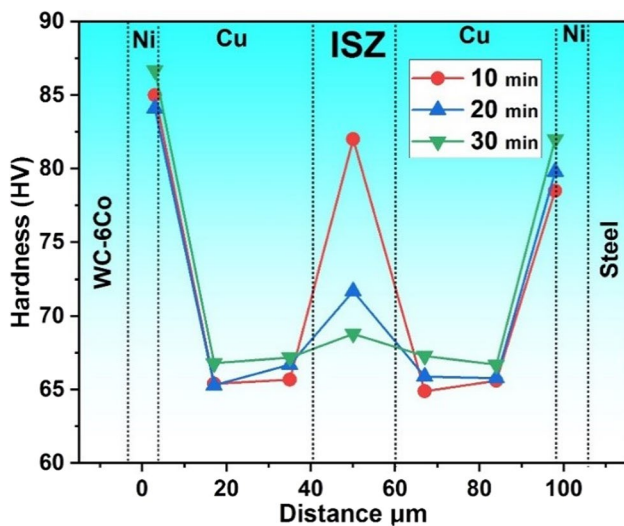


Fig. 10 The micro hardness profile in width of the WC-6Co/1045 steel TLP bonded joints at 650°C for different bonding times

3.2.2 Shear strength

Figure 11 shows the shear strength of the joints as a function of the bonding time. At the lowest bonding time (10 min), the shear strength is at its minimum. This is associated with the formation of the aforementioned brittle double-phase microstructure of $\delta + (\text{Cu})$ in the joint area as a result of inadequate bonding time. By prolonging the bonding time to 20 min, the atomic penetration of the molten indium interlayer is promoted, resulting in

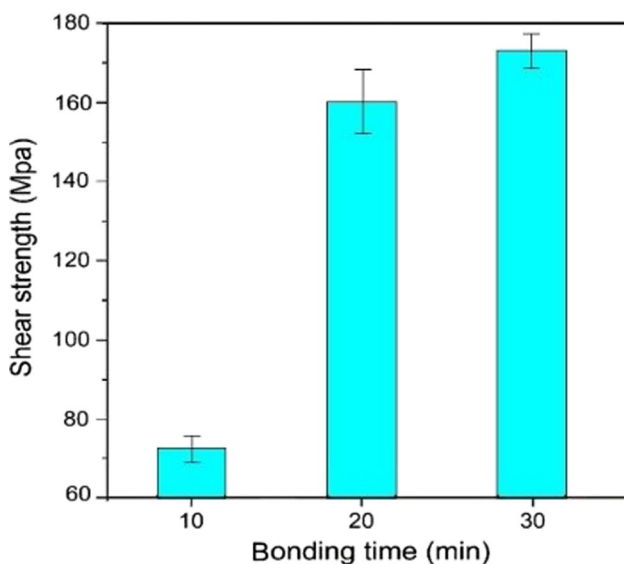


Fig. 11 Effect of bonding time on shear strength of the joints (TLP temperature is 650°C)

the isothermal formation of the Cu-In solid solution with less than 6 atomic percent in the TLP joining zone. This corresponds to an increase in joint shear strength from approximately 73 to 160 MPa. According to Fig. 11, the maximum shear strength values for the TLP joints were obtained at 173 MPa for samples bonded for 30 min. This increase is associated with the homogenization of the isothermally formed (Cu) solid solutions within these samples.

3.3 Fractography

The XRD spectra of fracture surfaces of joints (WC-6Co side) bonded for 10 min (Fig. 12a) shows the presence of both δ and (Cu) phases at the fracture surface. This not only indicates incomplete isothermal solidification of copper solid solution but also crack propagation through the double-phase microstructure. The higher intensity of (Cu) peaks compared to $\text{Cu}_7\text{In}_3(\delta)$ suggests that in significant portion of the joint area, copper solid solution was isothermally solidified while in the remaining areas β phase with higher concentration of indium solidified which decomposed to $\delta + (\text{Cu})$ at 574°C. The SEM image of the fracture surface of the sample bonded for 10 min (Fig. 12a) illustrates brittle fracture, unlike the SEM images from the surfaces of specimens bonded for 20 and 30 min (Fig. 12b and c), which show dimples and severe plastic deformation, indicating ductile fracture. Figure 12b and c also illustrates the X-ray diffraction spectra obtained from the fracture surfaces (WC-6Co sides) of specimens bonded for 20 and 30 min, showing only copper peaks. According to EDS analyses of the fracture surfaces, they should be mainly copper solid solutions with less than 1% indium (atomic percent).

4 Conclusion

This study investigated the effect of bonding time on the strength of dissimilar WC-Co/steel joints fabricated by the transient liquid phase (TLP) bonding method at 650°C using an indium interlayer. The significant results are summarized as follows:

- (i) Dual-phase microstructure of $\delta + (\text{Cu})$ was detected in samples bonded for 10 min at 650°C which indicates that 10 min was not enough for isothermal solidification of copper solid solution with 4 atomic percent indium. However, as bonding temperature prolonged to 20 min, a single phase solid solution of Cu(In) was isothermally solidified with 5.21% indium concentration. Further, prolonging bonding time to 30 min led to lower concentration of 3.15% indium (atomic present).

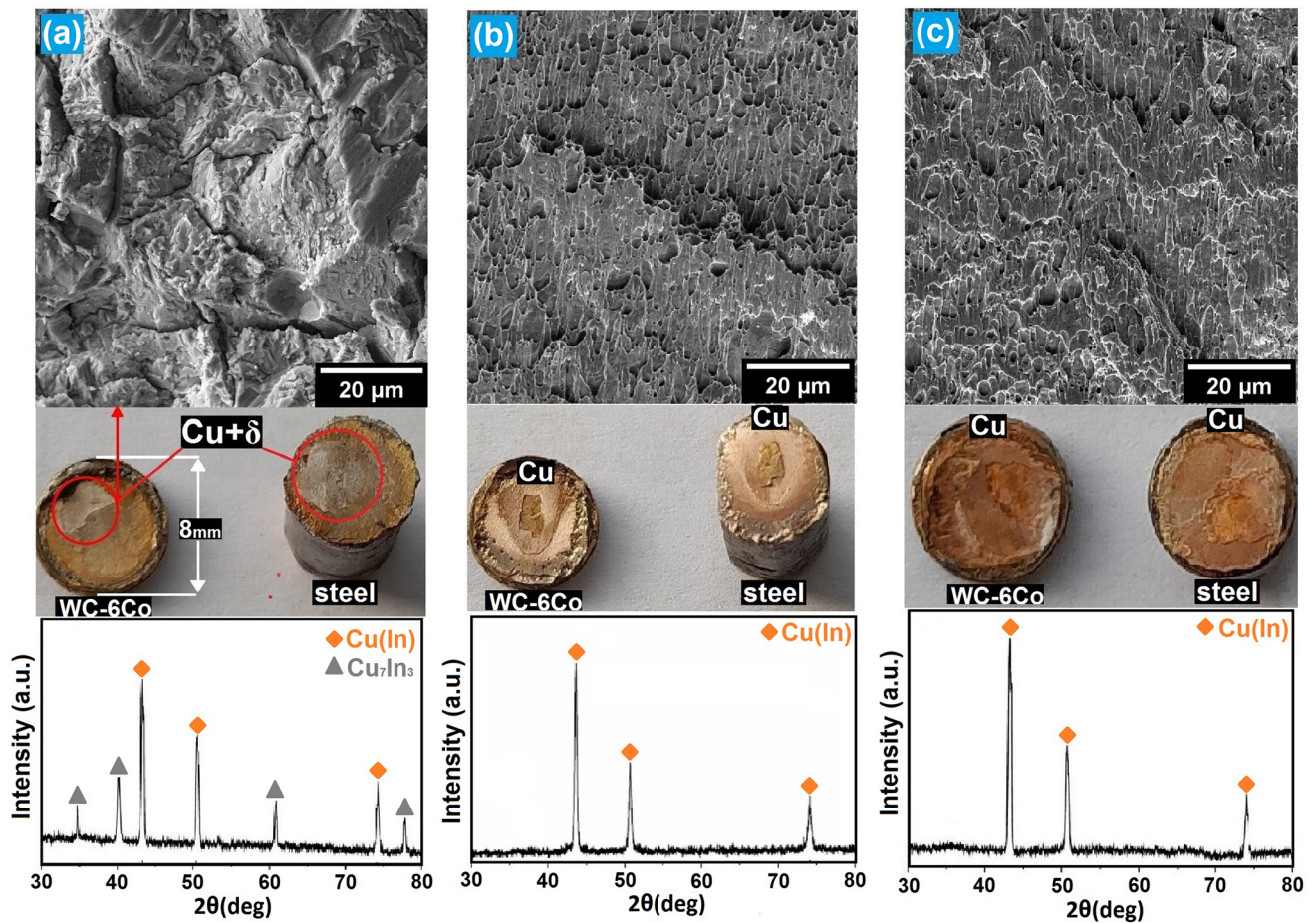


Fig. 12 SEM micrographs and X-ray diffraction spectra of the fracture surface (WC–Co side) of TLP joints formed at 650°C for (a) 10, (b) 20, and (c) 30 min

- (ii) Proper selection of TLP bonding parameters (a bonding time of 30 min with a 5- μm indium interlayer) promotes the formation of a sound and homogeneous (Cu) solid solution without the formation of destructive intermetallic compounds in the joint area.
- (iii) Through TLP processing at 650°C for 30 min, the remelting point of the formed Cu–In solid solution with 3.15% indium (atomic percent) in the joint area reached above 900°C based on a Cu–In phase diagram.
- (iv) By prolonging the bonding time from 10 to 30 min, shear strength raised from 73 to 173 MPa. Lower strength of the joint bonded in 10 min was attributed to brittle structure of Cu_7In_3 which was detected at the fracture surface of the joint bonded in 10 min.
- (v) TLP bonding for 30 min, with full dimple features in the fracture surface, exhibits a typical ductile fracture mode in the joint area.

Data availability The data used to support the findings of this study are included within the article.

Declarations

Competing interests The authors declare no competing interests.

References

- Upadhyaya GS (2001) Materials science of cemented carbides—an overview. *Mater Des* 22(6):483–489. [https://doi.org/10.1016/S0261-3069\(01\)00007-3](https://doi.org/10.1016/S0261-3069(01)00007-3)
- Bonny K, De Baets P, Perez Y, Vleugels J, Lauwers B (2010) Friction and wear characteristics of WC–Co cemented carbides in dry reciprocating sliding contact. *Wear* 268(11–12):1504–17. <https://doi.org/10.1016/j.wear.2010.02.029>
- Chen H, Feng K, Wei S, Xiong J, Guo Z, Wang H (2012) Microstructure and properties of WC–Co/3Cr13 joints brazed using Ni

- electroplated interlayer. *Int J Refract Metal Hard Mater* 1(33):70–74. <https://doi.org/10.1016/j.ijrmhm.2012.02.018>
4. Chen H, Feng K, Xiong J, Guo Z (2013) Characterization and stress relaxation of the functionally graded WC–Co/Ni component/stainless steel joint. *J Alloy Compd* 25(557):18–22. <https://doi.org/10.1016/j.jallcom.2012.12.152>
 5. Zhang X, Liu G, Tao J, Guo Y, Wang J, Qiao G (2018) Brazing of WC–8Co cemented carbide to steel using Cu–Ni–Al alloys as filler metal: microstructures and joint mechanical behavior. *J Mater Sci Technol* 34(7):1180–1188. <https://doi.org/10.1016/j.jmst.2017.11.040>
 6. Cao J, Liu J, Song X, Lin X, Feng J (2014) Diffusion bonding of TiAl intermetallic and Ti3AlC2 ceramic: interfacial microstructure and joining properties. *Mater Des* 1980–2015(56):115–21. <https://doi.org/10.1016/j.matdes.2013.10.074>
 7. Lei Y, Hu SP, Yang TL, Song XG, Luo Y, Wang GD (2020) Vacuum diffusion bonding of high-entropy Al0.85CoCrFeNi alloy to TiAl intermetallic. *J Mater Process Technol* 278:116455. <https://doi.org/10.1016/j.jmatprotec.2019.116455>
 8. Jianxin D, Hui Z, Ze W, Yunsong L, Jun Z (2012) Friction and wear behaviors of WC/Co cemented carbide tool materials with different WC grain sizes at temperatures up to 600 C. *Int J Refract Metals Hard Mater* 31:196–204. <https://doi.org/10.1016/j.ijrmhm.2011.11.003>
 9. Zhang JX, Chandel RS, Chen YZ, Seow HP (2000) Effect of residual stress on the strength of an alumina–steel joint by partial transient liquid phase (PTLP) brazing. *J Mater Process Technol* 122(2–3):220–5. [https://doi.org/10.1016/S0924-0136\(02\)00010-9](https://doi.org/10.1016/S0924-0136(02)00010-9)
 10. Habibi F, Samadi A, Nouri M (2023) Microstructural evolution during low-temperature brazing of WC-Co cemented carbide to AISI 4140 steel using a silver-based filler alloy. *Int J Refract Metal Hard Mater* 1(116):106354. <https://doi.org/10.1016/j.ijrmhm.2023.106354>
 11. Amelzadeh M, Mirsalehi SE (2018) Influence of braze type on microstructure and mechanical behavior of WC-Co/steel dissimilar joints. *J Manuf Process* 1(36):450–458. <https://doi.org/10.1016/j.jmapro.2018.10.015>
 12. Amelzadeh M, Mirsalehi SE (2019) Dissimilar vacuum brazing of cemented carbide to steel using double-layer filler metals. *J Manuf Process* 1(47):1–9. <https://doi.org/10.1016/j.jmapro.2019.09.015>
 13. Zhang XZ, Liu GW, Tao JN, Shao HC, Fu H, Pan TZ, Qiao GJ (2017) Vacuum brazing of WC–8Co cemented carbides to carbon steel using pure Cu and Ag–28Cu as filler metal. *J Mater Eng Perform* 26:488–494. <https://doi.org/10.1007/s11665-016-2424-6>
 14. Schwartz M (1992) Mechanical properties of ceramics. Handbook of Structural Ceramics. McGraw-Hill
 15. Klaasen H, Kübarssepp J, Laansoo A, Viljus M (2010) Reliability of dual compounds “carbide composite+ steel” produced by diffusion welding. *Int J Refract Metal Hard Mater* 28(5):580–586. <https://doi.org/10.1016/j.ijrmhm.2010.03.005>
 16. Lemus-Ruiz J, Avila-Castillo JJ, García-Estrada R (2007) WC/stainless steel joints produced by direct diffusion bonding using a Ni-Foil interlayer. *Mater Sci Forum Trans Tech Publ Ltd* 560:53–57. <https://doi.org/10.4028/www.scientific.net/MSF.560.53>
 17. Feng K, Chen H, Xiong JI, Guo Z (2013) Investigation on diffusion bonding of functionally graded WC–Co/Ni composite and stainless steel. *Mater Des* (1980-2015) 46:622–6. <https://doi.org/10.1016/j.matdes.2012.11.006>
 18. Barrena MI, De Salazar JG, Matesanz L (2010) Interfacial microstructure and mechanical strength of WC–Co/90MnCrV8 cold work tool steel diffusion bonded joint with Cu/Ni electroplated interlayer. *Mater Des* 31(7):3389–3394. <https://doi.org/10.1016/j.matdes.2010.01.050>
 19. Li SW, Shi JM, Xiong JT, Peng Y, Ren J, Zhang FS, Li J (2021) Microstructural characteristics and mechanical properties of WC-Co/steel joints diffusion bonded utilizing Ni interlayer. *Ceram Int* 47(4):4446–4454. <https://doi.org/10.1016/j.ceramint.2020.09.157>
 20. Guo Y, Wang Y, Gao B, Shi Z, Yuan Z (2016) Rapid diffusion bonding of WC-Co cemented carbide to 40Cr steel with Ni interlayer: effect of surface roughness and interlayer thickness. *Ceram Int* 42(15):16729–16737. <https://doi.org/10.1016/j.ceramint.2016.07.145>
 21. Li S, Li Z, Chen Y, Zu Y, Xiong J, Zhang F, Li J (2022) Microstructural evolution and mechanical properties of diffusion bonding WC-Co cemented carbide to steel using Co and composite Ni/Co interlayers. *Int J Refract Metal Hard Mater* 1(103):105736. <https://doi.org/10.1016/j.ijrmhm.2021.105736>
 22. Brochu M, Pugh MD, Drew RA (2004) PTLPB of Si3N4 to FA-129 using nickel as a core interlayer. *Int J Refract Metal Hard Mater* 22(2–3):95–103. <https://doi.org/10.1016/j.ijrmhm.2004.01.003>
 23. Sangha SP, Jacobson DM, Peacock AT. Development of the copper-tin diffusion-brazing process. *Welding Journal*. 1998 Oct 1; 77: 432-s.
 24. Cook GO III, Sorensen CD (2011) Overview of transient liquid phase and partial transient liquid phase bonding. *J Mater Sci* 46(16):5305–5323. <https://doi.org/10.1007/s10853-011-5561-1>
 25. Guo Y, Gao B, Liu G, Zhou T, Qiao G (2015) Effect of temperature on the microstructure and bonding strength of partial transient liquid phase bonded WC–Co/40Cr joints using Ti/Ni/Ti interlayers. *Int J Refract Metal Hard Mater* 1(51):250–257. <https://doi.org/10.1016/j.ijrmhm.2015.04.018>
 26. Zeidabadinejad H, Rafiei M, Ebrahimzadeh I, Omid M, Naeimi F (2023) Microstructural evolutions and mechanical properties of TLP-bonded WC-Co/St52 with copper interlayer. *Weld World* 67(10):2411–2421. <https://doi.org/10.1007/s40194-023-01562-y>
 27. Chen SJ, Tang HJ, Jing XT (2009) Transient liquid-phase bonding of T91 steel pipes using amorphous foil. *Mater Sci Eng, A* 499(1–2):114–117. <https://doi.org/10.1016/j.msea.2007.11.133>
 28. Subramanian PR, Laughlin DE (1989) The Cu–In (copper-indium) system. *Bull Alloy Phase Diagr* 10(5):554–68. <https://doi.org/10.1007/BF02882415>

Publisher's Note Springer Nature remains neutral with regard to jurisdictional claims in published maps and institutional affiliations.

Springer Nature or its licensor (e.g. a society or other partner) holds exclusive rights to this article under a publishing agreement with the author(s) or other rightsholder(s); author self-archiving of the accepted manuscript version of this article is solely governed by the terms of such publishing agreement and applicable law.